BULLETIN OF THE CHEMICAL SOCIETY OF JAPAN, VOL. 46, 2728—2734 (1973)

# The Magnetic Properties of Verdazyl Free Radicals. III.[1] The Anomalous Magnetic Behavior of Symmetrical Triphenylverdazyl

Nagao AZUMA,* Jun YAMAUCHI,** Kazuo MUKAI,*** Hiroaki OHYA-NISHIGUCHI,* and Yasuo DEGUCHI*

*Department of Chemistry, Faculty of Science, Kyoto University, Sakyo-ku, Kyoto 606
**The Institute for Chemical Research, Kyoto University, Uji, Kyoto 611
***Department of Chemistry, Faculty of Science, Ehime University, Matsuyama, Ehime 790

(Received February 7, 1973)

The static magnetic susceptibility and the ESR spectra from 1.6 to 300 K have been measured on a powder sample of the titled free radical. The broad maximum in the susceptibility which indicates an antiferromagnetic interaction has been observed at 6.9 K. The broadening of the ESR absorption line and the shift of the *g*-value have been found in the temperature region below $T_{max}$, in which the susceptibility reached its round maximum. There appeared anomalies in the slope of the susceptibility, the linewidth, and the *g*-value *versus* temperature curves in the vicinity of 1.7 K. These anomalies may imply a magnetic-phase transition from the short-range ordered state to the long-range ordered state at about 1.7 K. The existence of a ferromagnetic interaction between the magnetic chains in the triphenylverdazyl radical solid is discussed on the basis of the susceptibility, the spin distribution, and the crystal structure. It is understood qualitatively that the radical with a negative spin density has a latent ferromagnetic interaction in or between the magnetic chains, and that the obsrevation of this interaction greatly depends upon the molecular and crystal structure.

At a low temperature a number of free radical solids exhibit broad maxima in their susceptibilities which indicate an antiferromagnetic interaction between unpaired electrons in the radicals. In the case of neutral organic radicals, the magnetic behavior has been explained on the basis of magnetic linear chain models, where the linear Heisenberg and the one-dimensional Ising models have been commonly employed. On the other hand, all the organic free radicals show practically isotropic *g*-values very close to the free electron value. This implies a small spin-orbit interaction due to the quenching of the orbital angular momentum; as a result, one may take into account an isotropic exchange inter-

1) Part I: K. Mukai, N. Azuma, and K. Ishizu, This Bulletin, **43**, 3618 (1970).

action and a smaller magnetic dipolar one in order to interpret the magnetic data. Therefore, the appropriate model for discussing the magnetic behavior of free radicals may not be of the Ising-type with extremely anisotropic spins, but the Heisenberg model, with the isotropic exchange interaction; this model is employed in the present case. The one-dimensionality of the magnetic structure in the free radical solids may be acceptable, firstly, because the low symmetry of the crystal structure,[2-5] which, in turn, results in the small coordination number, $z$, of the unpaired electrons, where the linear chain $z=2$, and secondly, because of the uniaxial angular dependence of the $p_z\pi$-orbitals occupied by the unpaired electrons. In fact, we have found neither two- nor three-dimensional magnetic lattice in any organic radical solid, although Duffy *et al.*[6] proposed a magnetic quadratic-layered structure for di-*p*-anisyl nitroxide (DANO) in accordance with the crystal quadratic layer sub-lattice, which consists of molecular centers,[3] but with no regard for the angular dependence of the orbitals.[7]

It is well known theoretically[8] that the isolated magnetic linear chains do not show any sharp magnetic phase transition, but, a rather broad maximum susceptibility, and that, in the presence of a small interaction between the chains, the phase transition from a short-range ordered state to a long-range ordered state may occur. This magnetic phase transition has thus far been considered to be found in the complex of 1,3-bisdiphenylene-2-phenylallyl with benzene (BDPA-*Bz*)[7,9,10] and in 1,3-bisdiphenylene-2-*p*-chlorophenylallyl (*p*-Cl–BDPA).[7,11] The present paper will deal with 1,3,5-triphenylverdazyl (TPV), the magnetic measurements of which show the possible existence of the long-range ordering and whose crystal structure has been determined recently.[2]

If the crystal structure is known, one can carry out more detailed experiments to study minutely the magnetism of the radical solid. Unfortunately, the crystal structure of neither BDPA-*Bz* nor *p*-Cl–BDPA has been solved. It is also of much interest to relate the magnetic properties of radicals to their crystal structures and to examine the exchange interaction mechanism. In this paper we would like to describe the magnetic behavior of the titled radical and discuss the magnetism of TPV from the standpoints of exchange interaction, spin density, and the crystal structure. In the last section of discussion, the magnetism of the galvinoxyl radical will be discussed from the present point of view.

## Experimental

The sample was prepared by the method of Kuhn and Trischmann and was purified a few times through recrystallization from a mixture of acetone and methanol.[12] The melting point, which ranged from 142.0 to 142.5 °C, was found to agree well with the value in the literature. The results of the elementary analysis for carbon, hydrogen, and nitrogen were in good accord with the calculated values (Found: C, 76.43; H, 5.52; N, 17.94%.) The ESR spectrum in 2-methyltetrahydrofuran (2-MeTHF) *in vacuo* appeared in nine lines, with a line separation of 5.8 Gauss which can be assigned as the hyperfine coupling constant of four nearly equivalent nitrogen nuclei, and which is close to the value measured in a benzene solution and reported in the literature.

The magnetic susceptibilities from 1.6 to 300 K were measured on powder samples prepared independently in a heterogeneous magnetic field up to 8.8 kOe by means of a magnetic torsion balance described elsewhere.[13] The temperatures were determined using a calibrated AuCo–Cu thermocouple and a carbon resister. Manganese Tutton salt was used for the calibration of the thermometers as well as the product of the magnitude times the gradient of the magnetic field.

The ESR absorption spectra were observed on powder samples from 1.7 to 4.2 K and at the temperature of liquid nitrogen and at room temperature using a JES-ME-type spectrometer with an 80 Hz-field modulation. The temperatures were determined by means of the vapor pressures of liquid helium. An aqueous solution of peroxylamine disulfonate was used as the standard for the estimation of the $g$-value at room temperature. $Mn^{2+}$ in MgO was taken as the second standard for the $g$-value measurement at lower temperatures and as a field-calibrating material.

## Results

*Susceptibility.* The data have been corrected for the diamagnetic contribution using Pascal's constants.[14] The absolute molar susceptibility, $\chi_M$, corrected for diamagnetism, complies with Curie-Weiss law with a negative Weiss constant, $\theta=-8$ K, in the higher-temperature region. The susceptibility, however, deviates from the Curie-Weiss law at lower temperatures, and it shows a broad maximum with a value of $\chi_{max}=203\times10^{-4}$ emu/mol at a temperature of $T_{max}=6.9$ K. When the temperature is lowered further, the susceptibility decreases comparatively slowly towards a minimum and then, as is shown in Fig. 1, unexpectedly increases again just after passing through the minimum point at $T_n=1.7$ K, where a discontinuity in the slope of the susceptibility is observed. The finite susceptibility at 0 K is roughly estimated as to be equal to $\chi_{T=0}=170\times10^{-4}$ emu/mol by the extrapolation of the $\chi_M$ *versus* $T$ curve between the $T_{max}$ and $T_n$ temperatures. The radical concentration, as determined from the susceptibility in the temperature region above

2) D. E. Williams, *J. Amer. Chem. Soc.*, **91**, 1243 (1969); preprint (to appear in *Acta Crystallogr.*).
3) A. W. Hanson, *Acta Crystallogr.*, **6**, 32 (1953).
4) D. E. Williams, *Mol. Phys.*, **16**, 145 (1969).
5) J. Lajzerowicz-Bonneteau, *Acta Crystallogr.*, **B24**, 196 (1968); D. E. Williams, *J. Amer. Chem. Soc.*, **89**, 4280 (1967).
6) W. Duffy, Jr., D. L. Strandburg, and J. E. Deck, *Phys. Rev.*, **183**, 2218 (1969).
7) J. Yamauchi, This Bulletin, **44**, 2301 (1971).
8) L. Onsager, *Phys. Rev.*, **65**, 117 (1944); H. E. Stanley and T. A. Kaplan, *Phys. Rev. Lett.*, **17**, 913 (1966).
9) W. O. Hamilton and G. E. Pake, *J. Chem. Phys.*, **39**, 2694 (1963).
10) W. Duffy, Jr., J. F. Dubach, P. A. Pianetta, J. F. Deck, D. L. Strandburg, and A. R. Miedema, *ibid.*, **56**, 2555 (1972).
11) J. Yamauchi, K. Adachi, and Y. Deguchi, *Chem. Lett.*, **1972**, 733 (1972); *J. Phys. Soc. Jap.*, **35**, 443 (1973).
12) R. Kuhn and H. Trischmann, *Monatsh. Chem.*, **95**, 457 (1964).
13) M. Mekata, *J. Phys. Soc. Jap.*, **17**, 796 (1962).
14) P. W. Selwood, "Magnetochemistry," Interscience Publisher, New York (1956).

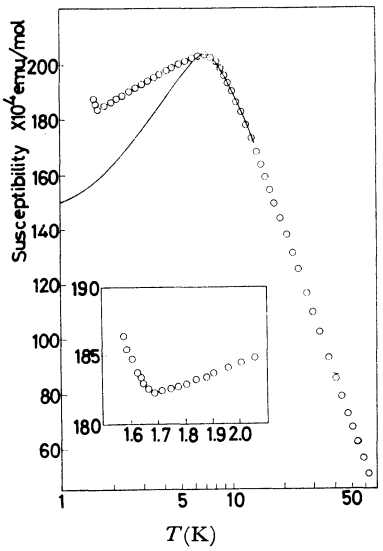


Fig. 1. Magnetic molar susceptibility of TPV.
Solid line represents the theoretical susceptibility calculated by the linear Heisenberg model. The inset shows the susceptibility at temperatures below 2 K.

77 K, was found to be 100% within the limit of experimental error. The reproducibility of the data was confirmed by comparing them with the data of samples prepared independently.

*ESR.* The ESR absorption spectrum shows a single line with an exchange-narrowed Lorentzian shape. In the higher-temperature region above $T_{max}$, the $g$-value was found to be practically isotropic, close to the free electron value and independent of the temperature. However, the $g$-value rapidly increases because of the anisotropic contribution in the lower-temperature region below $T_{max}$. The estimated $g$-value *versus* temperature curve is shown in Fig. 2. The temperature-dependent $g$-value of the another verdazyl radical, which exhibits a broad maximum susceptibility at *circa* 12 K but which is subjected to no long-range ordering in the available temperature range, is shown in the same figure for the sake of comparison.[15] The linewidth, which was taken to be the peak-to-peak linewidth ($\Delta H_p$) of the first derivative of the resonance spectrum, probably starts to increase rapidly as the temperature is decreased below about $T_{max}$. The increase becomes more rapid as the temperatures approach

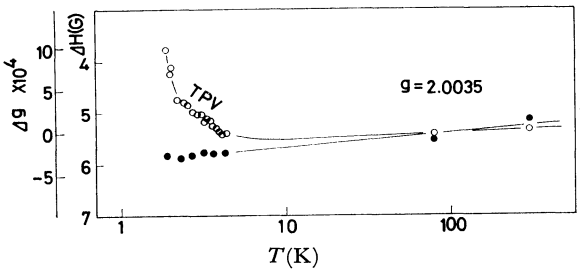


Fig. 2. Temperature dependent $g$-value of TPV.
$\Delta H$ stands for the shift of resonance field from the standard resonance field of $Mn^{2+}$ in MgO (Gauss). Solid circles represent the $g$-value of the referred sample.

15) unpublished data.

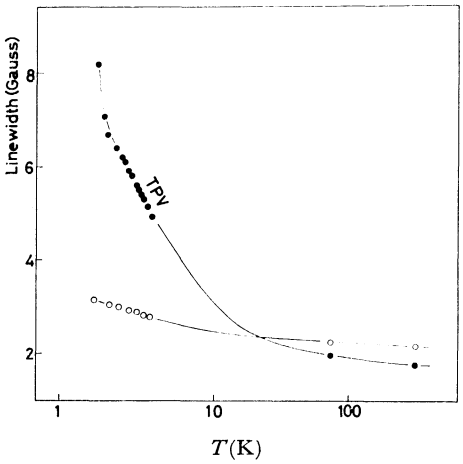


Fig. 3. Linewidth of TPV.
Open circles stand for the linewidth of the referred sample.

$T_n$=1.7 K, which may be closely related to the increase in the $g$-value. The temperature dependences of the linewidths of TPV and the aforementioned radical are compared in Fig. 3.

## Discussion

*Susceptibility.* One of the features of the susceptibility is, as may be seen in Fig. 1, that a finite susceptibility at 0 K seems to be left; this suggests a Heisenberg-type linear exchange interaction between unpaired electrons. This agrees well with the isotropic character of the $g$-factor. Therefore, the suceptibility may be described with neither Ising models[16,17] nor an exchange-coupled model.[18]

Therefore, we considered the linear Heisenberg model with isotropic exchange interaction, following the numerical calculation made by Bonner and Fisher.[19] The procedure of estimating the susceptibility has been described elsewhere.[7] The susceptibility gives an excellent fit to the value observed using $J/k=-5.4$ K, without any extra parameter such as a purity factor, in the temperature region above 6 K. However, the observed susceptibility deviates upwards from the theoretical value as the temperature is decreased below $T_{max}$. The value of $\chi_{max}/\chi_{T=0}$, being independent of the $J$ parameter, is actually 1.2, while the theory predicts 1.45. On the other hand, the Weiss constant of $-8$ K, which agrees well with the value measured preliminarily in the temperature range above 77 K,[20] is larger in its absolute value than the theoretical one of 0.78 $T_{max}$, in contrast with the case of the product of $T_{max}$ times $\chi_{max}$ 0.141 and 0.140 emu K/mol for the theoretical and observed values respectively. These two relationships are also independent of the $J$ parameter.

16) J. W. Stout and R. C. Chisholm, *J. Chem. Phys.*, **36**, 979 (1962).
17) M. Inoue, *Nippon Kagaku Zasshi*, **92**, 1 (1971).
18) B. Bleaney and K. D. Bowers, *Proc. Roy. Soc., Ser. A*, **214**, 451 (1952).
19) J. C. Bonner and M. E. Fisher, *Phys. Rev.*, **135**, A640 (1964).
20) R. Kuhn. F. A. Neugebauer, and H. Trischmann, *Monatsh. Chem.*, **97**, 525 (1966).

Two coexistent interactions may make possible an interpretation of this feature. One of them rules predominantly and antiferromagnetically over the magnetism in the higher-temperature region and behaves one-dimensionally; the other is weaker than the former and is negligible in the higher-temperature region, but its latent ferromagnetic nature to tie up chain with chain is significant at temperatures below $T_{max}$. When the ferromagnetic contribution is adequately subtracted from the observed susceptibility, $T_{max}$ may be shifted towards a higher temperature; the value of $|\theta|/T_{max}$ may then decrease to the theoretical value. One might suspect that the low-temperature discrepancy could be attributed to radical impurities, such as a defect in the crystal structure or a terminal spin contribution in the magnetic chain. However, the sample with a lower radical concentration (92%) shows a susceptibility quite similar to that of the pure sample except for the slight decrease in $T_{max}$ (6.6 K), while a pure sample prepared independently gives an excellent agreement with the data of the other pure sample. Thus, the impurity contribution can not explain the discrepancy. Even if a two-dimensional antiferromagnetic model is taken into account, this low-temperature residual susceptibility may also be almost unchanged, although for the two-dimensional Heisenberg antiferromagnet neither an exact nor appropriate solution reliable at tempreatures below $|J|/k$ is yet known.

The presence of the interchain magnetic interaction accounts for the magnetic-phase transition from the short-range ordered state to the long-range ordered state, a transition which is inferred from the discontinuity in the slope of the susceptibility and the anomalies in the linewidth and $g$-value curves in the vicinity of 1.7 K.

*ESR.* Recently, Nagata *et al.* reported the short-range-order effects on the $g$-values in the Heisenberg linear chain antiferromagnets containing $Mn^{2+}$ ion ($S=5/2$).[21] By introducing a small magnetic dipolar interaction and single-ion $D$-term, both of a uniaxial symmetry referred to the linear-chain direction, they classically estimated the simple relations between the anisotropies of the $g$-value and the susceptibility. The relationships were as follows:

$$\Delta g_{//}/g = (\chi_{//}-\chi_{\perp})/\chi_{//}, \quad (1)$$

$$\Delta g_{\perp}/g = (\chi_{\perp}-\chi_{//})/(2\chi_{\perp}). \quad (2)$$

When we assume the following relation for the powder sample:

$$\Delta g_{iso} = (\Delta g_{//}+2\Delta g_{\perp})/3, \quad (3)$$

then Eqs. (1) and (2) give this expression:

$$(1/g)\Delta g_{iso} = -(\chi_{//}-\chi_{\perp})^2/(3\chi_{//}\chi_{\perp}). \quad (4)$$

Eq. (4) indicates that, under their conditions, the $g$-value observed on the powder sample decreases with a decrease in the temperature if the anisotropic susceptibility is produced. We would like, however, to suggest that the essential part of Eqs. (1)—(4) lies in neither the sign nor the exact amplitude of the $g$-value shift, but in their suggestion that the anisotropic $g$-value reflects the anisotropy in susceptibility. Therefore, in comparison with the two curves shown in Fig. 2, the low-temperature $g$-value shift of TPV can be attributed to the susceptibility anisotropy in its solid. The striking shift in the temperature region below 2 K may imply the evolution of a severe change in the spin system in the vicinity of that temperature and may provide additional evidence of the phase transition at any temperature below 2 K. The sign of the $g$-value shift of TPV has to be subjected to an intense examination, together with the anisotropy in the susceptibility.

Although no appropriate theory for the linewidth of free radicals has been established, one of the present authors has previously reported the temperature dependence of the ESR absorption linewidth on a number of free radicals.[7] He found that the short-range ordering, remarkably developed near $T_{max}$, can be observed on the increase in the ESR linewidth, because the line broadening corresponds to an increase in the correlation time of the exchange motion due to the magnetic short-range ordering. In the present case, the line broadening probably starts to increase significantly at a higher temperature than what would be expected from $T_{max}$ in view of the other data published.[7] This may be attributed to the precocious short-range ordering and may provide another support for the interchain ferromagnetic interaction derived from the susceptibility measurements. The broadening-out of the resonance line in the temperature region below 2 K may also be associated with the onset of the magnetic-phase transition in the neighborhood of that temperature, since, as the phase-transition temperature is approached, the increased spin-spin correlation results in the decreased exchange-narrowing of the linewidth.

*Spin Distribution in the Molecule.* The magnetic properties of free radicals with a delocalized unpaired electron may be greatly affected by the spin distribution. The proton NMR spectrum of TPV in a solution has exhibited well-resolved absorption lines.[22] Using the simple form of the McConnell relationship:[23]

$$a_i = -Q\rho_i, \quad Q = 23.7 \text{ Gauss},[24]$$

where $a_i$ is the isotropic hyperfine splitting of the $i$th proton and where $\rho_i$ is the spin density on the adjacent carbon atom, the spin densities on the carbon atoms were estimated, they are listed in Table 1. The McLachlan spin densities have been calculated and give a good agreement with the observed nitrogen hyperfine splitting of TPV.[23] Only the spin densities on the atoms with no adjacent hydrogen atom are also listed in the same table, because the McLachlan spin densities on aromatic rings do not always reproduce the proton splittings. The spin distribution in the table, together with the crystal structure to be considered in the next paragraph, will be discussed in connection with the magnetic structure of TPV.

*Crystal Structure.* According to the detailed crystallographic data which have been kindly supplied by

21) K. Nagata and Y. Tazuke, *J. Phys. Soc. Jap.*, **32**, 337 (1972); K. Nagata, Y. Tazuke, and K. Tsushima, *ibid.*, **32**, 1486 (1972).

22) P. Kopf, K. Morokuma, and R. Kreilick, *J. Chem. Phys.*, **54**, 105 (1971).

23) H. M. McConnell, *ibid.*, **24**, 764 (1956).

24) P. H. H. Fischer, *Tetrahedron*, **23**, 1939 (1967).

Table 1. Spin distribution

| Position[a)] | Density |
|---|---|
| N1, N5 | 0.1944 |
| N2, N4 | 0.2040 |
| C3 | —[b)] |
| C6 | −0.0461 |
| C7, C13 | −0.0345 |
| C8, C12, C14, C18 | 0.0473 |
| C9, C11, C15, C17, C20, C24 | −0.0179 |
| C10, C16 | 0.0505 |
| C19 | 0.0032 |
| C21, C23 | 0.0067 |
| C22 | −0.0131 |

a) Numbering system is shown in Fig. 4.
b) The spin density is omitted in view of its small value for the sake of simplicity.

Williams prior to publication,[2] the molecule of TPV has no symmetry element in its crystalline state, although those of the other two symmetrical verdazyls possess a mirror plane.[25] The small twist angles about the bonds connecting the *sym*-tetrazyl ring with the aromatic rings attached to the nitrogens are observed in all three of the verdazyls, while the respective *C*-phenyl ring is almost coplanar with the plane defined by the four nitrogens. The atomic deviation of all the aromatic ring carbons from the plane of the nitrogens is comparatively small for all the radicals. There is no essential difference among the molecular geometries of the three radicals, so that the molecules of the symmetrical verdazyls seem to be subjected mainly to intramolecular requirements or to steric and electronic effects. Therefore, it may be acceptable to assume that the electronic configuration as well as the molecular structure of TPV in its solid state are similar to those in solution, except for the effect of the largest exchange force in the crystal. The molecular structure and the numbering system of TPV are shown in Fig. 4.

The crystals of TPV belong to the orthorhombic system, with the space group of $P2_12_12_1$ and with these lattice parameters; $a=18.467$, $b=9.854$, and $c=8.965$ Å. Figure 5 shows the mutual arrangement of the molecules; the numbers are used to show the molecular positions. The number of the intermolecular approaches less than 4.0 Å from the **1** molecule to those at the other positions is 58, 39 vectors of which direct to the molecules at the **1′**, **2**, and **2′** positions. The other 19 approaches are randomly distributed on the other five molecules and include neither N···N nor C···N contact. The 39 intermolecular approaches are listed in Table 2. For each molecule four planes are defined—three phenyl-ring planes and the plane of the four nitrogens. C6 is assumed to be positioned on the nitrogen plane. The dihedral angle between the planes including the two atoms being examined into the interatomic distance is shown in the third column of the same table. The angle defined by an interatomic vector and the corresponding plane in the **1** molecule is listed in the fourth column of the table.

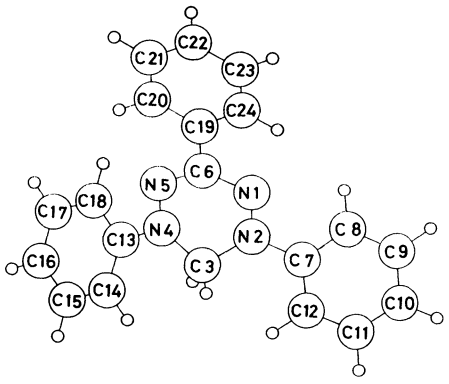


Fig. 4. Molecular structure and numbering system of TVP. C and N represent carbon and nitrogen atom, respectively. Small circles stand for hydrogen atoms.

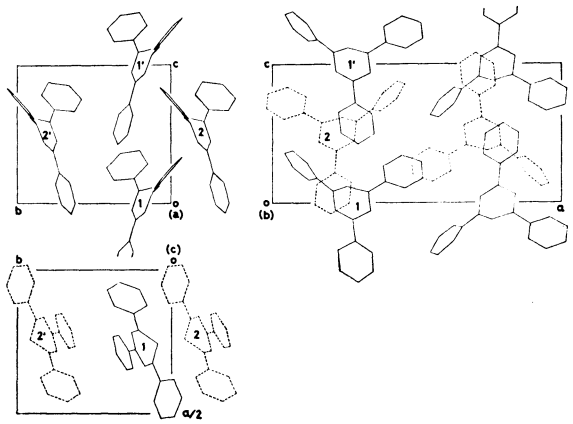

Fig. 5. Molecular packing of TPV.
(a), (b), and (c) correspond to the projections along the a-, b-, and c-axis, respectively. Numbers represent the molecular positions.

*Exchange Interaction and Spin Densities.* It is also important to discuss the relation between the signs of the apparent exchange integral and the spin density, because a problem may occur in certain solids of free radicals with a delocalized unpaired electron. Let us consider the following p-orbital exchange scheme:

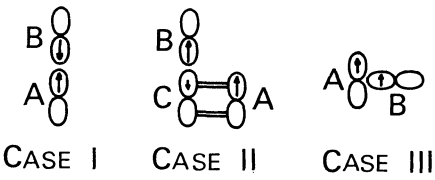


Case I corresponds to the general situation; that is, two p-orbitals on different molecules overlap with each other in the $z$-direction. In this case the favorable spin orientation is antiparallel or $J_{AB}$ is negative, because of the evolution of a small covalent bond. Case II illustrates the arrangement of the orbitals in the solid, which was referred to as a certain solid. The A and C orbitals belong to one molecule, and B, to the neighboring molecule. When the down-spin on the C orbital is polarized by the up-spin on the A orbital, the former spin can be related to the negative spin density. The overlap integral of the B and C orbitals results in a negative exchange integral, $J_{BC}$, so that a positive $J_{AB}$ may be observed. This mechanism is one way to explain the totally parallel spin

25) unpublished data.

orientation or the ferromagnetic interaction between unpaired electrons. Case III shows another variation of the orbital arrangement. The exchange integral in this case is positive but very small, because of the mutual orthogonality of the orbitals.[26,27] The magnitude of the apparent exchange interaction of these scheme may be proportional to the triple product of the spin densities on the two atoms concerned with the overalp and the corresponding exchange integral. This relation of the signs of the exchange integral and the spin densities is summarized and extended to a many-center problem by the following Hamiltonian:[26]

$$H^{AB} = -\mathbf{S}^A\mathbf{S}^B\sum_{ij}J_{ij}^{AB}\rho_i^A\rho_j^B, \quad (6)$$

where $\mathbf{S}^A$ and $\mathbf{S}^B$ are the total spins on Molecules A and B and where $\rho_i^A$ and $\rho_j^B$ are the $\pi$-spin densities on the $i$ and $j$ atoms of Molecules A and B. When the sum in Eq. (6) is positive, the apparent exchange interaction is ferromagnetic. The negative sign of the sum corresponds to an antiferromagnetic exchange interaction between unpaired electrons.

$$H^{AB} = -J_{AB}\mathbf{S}^A\mathbf{S}^B \quad (7)$$

When Eq. (6) is compared with Eq. (7), which corresponds to the Hamiltonian for the ordinary two-spin problem, then the sum in Eq. (6) can be named as the apparent exchange integral for a many-center problem.

*Possible Magnetic Structure.* The intermolecular distances less than 6.0 Å and the aforementioned angles were calculated in order to picture the magnetic structure of the TPV radical solid. Assuming that $J_{ij}^{AB}$ is simply proportional to the inverse of the interatomic distance ($d$) alone and that the negative unity for $d$=1 Å, Eq. (6) was applied to the data of the interatomic distance less than 4.0 Å and the corresponding spin densities listed in Table 1. The results are shown in Table 2, where the values in the fifth and sixth columns have been multiplied by $10^5$.

The molecules in the possible magnetic chain are related with each other by a twofold screw axis parallel to the c-axis. In this chain, the numbers of the intermolecular distances less than 4.0 Å from the atoms in the asymmetric unit molecule (Position **1**) to atoms in the nearest-neighboring (Position **2**) and the next nearest-neighboring (Position **1'**) molecules are 15 and 14 respectively; this is an interesting situation. The sum in Eq. (6) is negative for the nearest-neighboring molecule, while that for the next nearest-neighbor is positive, within the limits of the aforementioned broad assumption. The negative sign of the former sum indicates an antiferromagnetic interaction between the unpaired electrons, while the positive sign of the latter sum suggests a ferromagnetic interaction. However, these results may not indicate a competitive intrachain exchange interaction, but, rather, a cooperative totally antiferromagnetic interaction in the magnetic linear chain. It is suspected that the sum for the nearest-neighbor is estimated more highly than the sum for the next nearest-neighbor, taking account of the angular dependence of the exchange integral, $J_{ij}^{AB}$. The angle between the two orbitals may be inferred from the angles in the third and fourth columns of Table 2. We thus presume that the cooperative mechanism or the contribution of the second nearest-neighbor is too significant to neglect in this radical solid.

The number of the intermolecular approaches less than 4.0 Å associated with the nearest-neighboring molecule in the adjacent magnetic chain is 10, and the sum of these data gives a positive sign, which indicates

Table 2. Intermolecular distances (Å) and angles (degree), and the summation in Eq. (6)

| Atoms | $d$ | Dihedral angle | Direction angle | $\rho_i^A\rho_j^B$ | $J_{ij}^{AB}\rho_i^A\rho_j^B$ |
|---|---|---|---|---|---|
| *From Molecule* **1** *to Molecule* **2** | | | | | |
| C3–C6 | 3.93 | | | | |
| C3–C19 | 3.72 | | | | |
| C3–C20 | 3.80 | | | | |
| C11–C13 | 3.76 | 78.2 | 18.8 | 62.5 | −16.6 |
| C11–C18 | 3.80 | 78.2 | 0.5 | −84.6 | 22.5 |
| C12–N4 | 3.91 | 104.3 | 21.0 | 965.0 | −246.5 |
| C12–N5 | 3.60 | 104.3 | 4.8 | 920.0 | −255.5 |
| C12–C13 | 3.99 | 78.2 | 18.2 | −163.2 | 40.9 |
| C14–N1 | 3.42 | 104.3 | 16.4 | 920.0 | −269.0 |
| C14–N2 | 3.81 | 104.3 | 1.5 | 965.0 | −253.0 |
| C14–C6 | 3.79 | 104.3 | 32.9 | −218.0 | 57.5 |
| C14–C24 | 3.90 | 111.5 | 53.5 | −84.7 | 21.7 |
| C15–N1 | 3.68 | 104.3 | 32.6 | −348.0 | 94.6 |
| C15–N2 | 3.89 | 104.3 | 13.7 | −365.0 | 93.9 |
| C15–C7 | 3.94 | 97.3 | 3.0 | 61.8 | −15.7 |
| | | | *Sum* | 2630.8 | −725.2 |
| *From Molecule* **1** *to Molecule* **1'** | | | | | |
| N2–C22 | 3.68 | 7.5 | 53.4 | −267.0 | 72.5 |
| C3–C22 | 3.82 | | | | |
| N4–C22 | 3.86 | 7.5 | 49.5 | −267.0 | 69.2 |
| C7–C22 | 3.59 | 42.9 | 84.9 | 45.2 | −12.6 |
| C7–C22 | 3.54 | 42.9 | 72.9 | −23.1 | 6.5 |
| C8–C22 | 3.92 | 42.9 | 65.9 | −62.0 | 15.8 |
| C8–C23 | 3.66 | 42.9 | 67.8 | 31.6 | −8.6 |
| C9–C23 | 3.79 | 42.9 | 63.4 | −12.0 | 3.2 |
| C10–C23 | 3.81 | 42.9 | 62.7 | 33.8 | −8.9 |
| C11–C23 | 3.68 | 42.9 | 66.6 | −12.0 | 3.3 |
| C12–C22 | 3.91 | 42.9 | 66.9 | −62.0 | 15.9 |
| C12–C23 | 3.57 | 42.9 | 72.3 | 31.6 | −8.8 |
| C13–C21 | 3.78 | 33.5 | 73.1 | −23.1 | 6.1 |
| C14–C21 | 3.68 | 33.5 | 80.7 | 31.6 | −8.6 |
| | | | *Sum* | −554.4 | 145.0 |
| *From Molecule* **1** *to Molecule* **2'** | | | | | |
| N1–C22 | 3.89 | 39.6 | 53.5 | −254.5 | 65.5 |
| N1–C23 | 3.74 | 39.6 | 72.2 | 130.3 | −34.9 |
| C8–C19 | 3.90 | 68.5 | 42.3 | 15.1 | −3.9 |
| C8–C20 | 3.79 | 68.5 | 22.5 | −84.6 | 22.4 |
| C8–C21 | 3.73 | 68.5 | 6.1 | 31.7 | −8.5 |
| C8–C22 | 3.78 | 68.5 | 7.2 | −62.0 | 16.4 |
| C8–C23 | 3.85 | 68.5 | 24.8 | 31.7 | −8.2 |
| C8–C24 | 3.93 | 68.5 | 43.5 | −84.6 | 21.6 |
| C9–C20 | 3.79 | 68.5 | 22.5 | 32.1 | −8.5 |
| C24–C22 | 3.95 | 32.3 | 54.8 | 23.4 | −5.9 |
| | | | *Sum* | −221.4 | 56.0 |

a) Meanings of the figures are given in the text.

26) H. M. McConnell, *J. Chem. Phys.*, **39**, 1910 (1963).
27) J. Kanamori, *J. Phys. Chem. Solids*, **10**, 87 (1959).

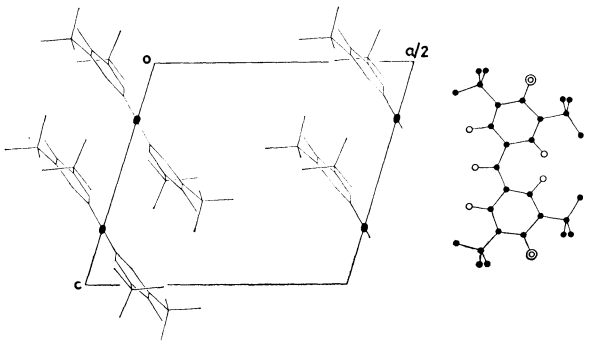


Fig. 6. Molecular packing and molecular structure of galvinoxyl radical. Solid ovals represent the diad axes. Solid circles stand for carbon atoms and doubled circles for oxygen atoms. Open circles represent hydrogen atoms. The methyl hydrogens in *tert*-butyl groups are not drawn.

a ferromagnetic interchain interaction. Thus, the intrachain antiferromagnetic and interchain ferromagnetic interactions inferred from the susceptibility measurement are qualitatively confirmed on the basis of the spin distribution and the crystal structure.

*Galvinoxyl Radical.* In order to confirm our proposal regarding the ferromagnetic interaction, let us consider the galvinoxyl radical solid, the susceptibility of which follows the Curie-Weiss law with a positive Weiss constant of 11 K above 83 K.[28] The crystal system of the radical solid is monoclinic, with a space group of C2/c, and with the cell dimensions of $a=23.78$, $b=10.87$, $c=10.69$ Å, and $\beta=106.6$ degrees.[4] Figure 6 shows the molecular packing, where the a-axis is drawn up to the half way mark. The molecule has a diad axis through the C–H bond in the methine group; this molecular twofold axis coincides with the crystallographic diad axis. The dihedral angel between the planes of the radical halves is 17 degrees. In Fig. 6, two methine carbons on the $a$-plane are positioned at (0.0, 0.03668, 0.25) and (0.0, −0.03668, 0.75); the other two methine carbons have the coordinates (0.5, 0.53668, 0.25) and (0.5, 0.46332, 0.75) respectively. Therefore, it can be said that this radical solid has a typical linear-chain magnetic structure along the c-axis, without any significant interchain interaction; therfore the above-mentioned susceptibility data may give information about its intrachain interaction alone. Within the chain, the intermolecular vectors which make angles from 70 to 90° (taken as an acute angle) with the phenyl plane and shorter than 5.0 Å were collected; the number of the vectors was 24. The spin densities were taken from Refs. 29 and 30. A procedure similar to that in the last section gives a positive sign for the sum in Eq. (6). Therefore, the comparatively large positive Weiss constant of 11 K may correspond to the ferromagnetic interaction caused by the overlap of a positive-spin-density-radical part with the negative-spin-density one in the neighboring molecule. It is interesting to notice that the qualitative magnetic behavior of two radical solids can be explained using Eq. (6).

28) K. Mukai, This Bulletin, **42**, 40 (1969).
29) B. Hakasson, *Acta Chem. Scand.*, **17**, 2281 (1963).
30) G. R. Luckhurst, *Mol. Phys.*, **11**, 205 (1966).

## Summary

The experimental results may be summarized as follows:
1) The susceptibility of TPV is well described by the linear Heisenberg model in the temperature region above 6 K, but deviates upwards from the theoretical one with a decrease in the temperature below 6 K and then exhibits a discontinuity in its slope at 1.7 K. The parameters derived from the susceptibility are $\theta=-8$ K, $T_{max}=6.9$ K, $\chi_{max}=203\times10^{-4}$ emu/mol, and $J/k=-5.4$ K. 2) The ESR absorption linewidth, which is associated with the correlation time of the exchange motion, increases in the vicinity of $T_{max}$ and broadens rapidly with a decrease in the temperature below 2 K. The temperature dependence of the $g$-value, which reflects the anisotropy in the susceptibility, is similar to that of the linewidth.

To summarize our interpretation of the results:
1) This radical solid may belong to the linear antiferromagnetic Heisenberg magnet, with a considerable ferromagnetic interaction between the chains. The discontinuing susceptibility at 1.7 K may imply a magnetic long-range ordering caused by the interchain ferromagnetic coupling. The pronounced increases in both the linewidth and the $g$-value below 2 K may be attributed to the critical fluctuation of electron spins in the neighborhood of the transition temperature. 2) The magnetic structure has been discussed on the basis of the spin distribution on the single molecule and the crystal structure. The possible linear chain is parallel to the c-axis, which is the shortest of the three orthorhombic axes. In this chain, the contribution of the second nearest-neighbor is significant and this is a ferromagnetic interaction which is cooperative with the antiferromagnetic one between the adjacent spins. The interchain interaction derived by our calculating procedure is ferromagnetic. 3) This magnetic structure can account for the qualitative experimental results of TPV. The method employed in the case of TPV was applied to the galvinoxyl radical solid and its positive Weiss constant of 11 K was attributed to the intrachain ferromagnetic interaction.

The authors would like to acknowledge the continuing guidance and encouragement of Professors Hideo Takaki and Mamoru Mekata of Kyoto University and Professor Kazuhiko Ishizu of Ehime University. They are also deeply indebted to Professor Yoshihiko Saito of the University of Tokyo for his helpful advice and for the use of considerable facilities in the determination of the crystal structures of the verdazyl radicals under consideration. They also thank Professor D. E. Williams of Louisville University, who supplied a preprint about the crystal structure of TPV and allowed them to reproduce the crystallographic figures of TPV and galvinoxyl radicals.